Combining Contact Forces and Geometry to Recognize Objects during Surface Haptic Exploration

Teng Sun, Junghwan Back, Hongbin Liu, *Member, IEEE**

***Abstract*—Enhancing haptic sensing allows more efficient control of interaction with unstructured and changing environments. Meanwhile, rich haptic information obtained during the interaction is useful for recognizing the environment. The haptic information contains distinctive physical features like friction, surface texture, local geometry, etc. However, how to combine these features for recognizing the environment is underexplored. Our previous work demonstrated that with accurate estimation of contact locations, and the direction and magnitude of the normal and tangential forces, a finger can follow unknown surfaces even with large changes in curvature while keeping a desired normal force. In this paper, we propose an object recognition method, using a multivariate Gaussian Bayesian classifier that collectively combines the haptic information, including friction coefficients and surface roughness, with the local geometry to recognize the object after surface haptic exploration. 18 objects with different materials and shapes were tested and results show that the method achieved a recognition accuracy of 92.3% on average. In addition, we compared the method with 6 other classifiers, and concluded that it is easier to use while having high accuracy. Most importantly it can show the levels of similarities between the features of different objects, and provide a causal explanation of the recognition accuracy. This paves a way towards active and adaptive exploration where highly efficient recognition can be realized by selectively probing the most distinguishable features.**

***Index Terms*—Haptics and Haptic Interfaces, Object Detection, Segmentation and Categorization**

I. Introduction

SENSE of touch is one of the most important pieces of information that human beings utilize to interact with surrounding objects and the environment, and to understand the objects being interacted with [1], [2], [3]. Similarly, it is expected to be essential for a robot to interact with and recognize an unstructured and changing environment. Surface haptic exploration has been attracting much attention in the research in this field [4], [5]. Humans can readily explore an unknown object's surface with their hands, adjusting the movements according to the material and shape of the object to explore smoothly and adaptively, and identify the object with the information gained through haptic exploration. To equip a robot with such ability, many researchers have tried to develop systems to acquire information about the object through haptic surface exploration [6], [7] and identify the objects by analyzing the information using methods of machine learning or classification [8], [9], [10], [11]. However, it is still challenging to use robots to carry out haptic surface exploration as humans can do, especially for objects with large geometry changes and different textures, due to the requirements of highly reactive and adaptive adjustments to maintain during the haptic interaction. In most of the previous works, the exploration procedure has been carried out by groping over a relatively flat surface of the object or by pressing [12], [13]. Moreover, researchers mostly focus on the friction and surface texture of the object. Jamali et al. [14] tried to classify material by tactile sensing using surface texture, and Song et al. [15] tried to predict slip by analyzing the friction ratio based on haptic surface exploration or only with geometry information obtained through haptic exploration [16], where the forces were only used for determining if contact occurred. However, to the best knowledge of the authors, the method of using the combination of the surface friction property and geometry for recognizing objects during haptic exploration has not been reported.

Recently, some studies have been presented trying to achieve smooth and adaptive surface explorations [17], [18], [19], [20], [21], [22], especially for discontinuous [23] and heterogeneous [24] surfaces. In our previous work [25], we introduced a contact-sensing algorithm for a robotic fingertip equipped with a 6-axis force/torque sensor to obtain the precise contact location information in real time. Based on this work, Back et al. [18] proposed a surface following control method using the contact location information to explore unknown objects with large changes in curvature while maintaining a relatively constant normal force, making it possible to get precise data of the forces and contact locations. In this paper, in order to fully utilize the haptic information gained through surface haptic exploration, we developed a novel object recognition method, which infers features of the friction coefficient, surface roughness, and local geometry with the obtained haptic information. The proposed method is in the form of a multivariate Gaussian Bayesian classifier that combines all the above features to recognize the explored objects.

All functionalities were implemented in ROS (Robot Operating System) and 18 objects with different materials and shapes were used to evaluate the performance of the designed

*Manuscript received September 10, 2017; Revised December, 20, 2017; Accepted February 11, 2018. This paper was recommended for publication by Editor Y. Yokokohji upon evaluation of the Associate Editor and Reviewers' comments. This work was supported by the EPSRC in the ESSENCE Project under Grant EP/N020421/1.

All authors are with the Centre for Robotics Research, King's College London, London WC2R 2LS, U.K. (e-mail: teng.sun@kcl.ac.uk).

Digital Object Identifier (DOI): see top of this page.

This article has been accepted for publication in a future issue of this journal, but has not been fully edited. Content may change prior to final publication. Citation information: DOI 10.1109/LRA.2018.2814083, IEEE Robotics and Automation Letters

method with their geometry known. In detail, for each object, 100 surface haptic explorations were conducted to train the classifier, followed by 50 recognitions to test the recognition accuracy. The experimental results show that the proposed classifier achieved a high accuracy of 92.3% on average.

II. Test Platform and Experimental Protocol

To study how to recognize an unknown object through surface haptic exploration, we created a test platform (Fig. 1). Implementing the control algorithm in [18], the robotic finger can maintain a constant contact normal force during surface haptic exploration without knowing the types and shapes of the objects. Moreover, during the haptic exploration, data processing and acquisition methods have been established to record the data, the sampling rate to capture the data generated during the exploration is 100hz.

The test platform mainly consists of a two-joint finger with DC motors and encoders embedded inside. A 6-axis force torque sensor (ATI Nano17, resolution 0.003N) is mounted inside a blue soft hemisphere made of silicone material (made by Ecoflex-50 with hardness Shore 00-50). We use a National Instruments PCIe-6320 data acquisition card to get sensor data at 16kHz and the ROS driver will get the data and publish the data at 100Hz. An experiment has been done to test the hysteresis of the soft fingertip, and results show that the tip has no hysteresis when the force applied on it is within 2.5N and the stiffness of the tip is about 2N/mm.

All the mechanical parts are made by 3D printing, shown in Fig. 1 (above). With the platform, the contact normal force f_n can be controlled with closed-loop control. We tested with mean(f_n) ≈ 0.35N, 0.45N, 0.55N, and Fig. 2 shows an example of the resultant forces. Also, in order to increase the DOF (degree of freedom) of the platform, the finger is attached to the UR-3 robotic arm. In this study, the arm will only rotate when necessary to relocate the finger relative to the explored object. The exploration velocity υ can also be controlled, and we test with the mean(υ) ≈ 35mm/s, 40mm/s, 45mm/s and 50mm/s. In our study, we simultaneously recorded the contact forces $\vec{\boldsymbol{F}} = [f_n, f_t]$ and contact locations $\overrightarrow{\boldsymbol{P_c}} = [p_x, p_y, p_z]$ during surface haptic exploration:

- Decide the target contact normal force and following velocity, and start the haptic exploration.
- Record normal forces f_n and tangential forces f_t simultaneously computed with the raw data from the force sensor each time when physical contact occurs between the finger and the object.
- Compute the contact locations $\overrightarrow{\boldsymbol{P_c}}$ on the tip with the contact equilibrium system equation proposed in [25] based on force/torque measured and transform that to base frame $\overrightarrow{\boldsymbol{P_O}}$ and record the trajectory T[$\overrightarrow{\boldsymbol{P_O}}$] of the contact locations after the exploration.

The main functionalities including motor control, sensor processing and object recognition are implemented in ROS using an Ubuntu installed PC (Intel® Core™ i7-2600 CPU @ 3.40GHz, 16G RAM) with a loop rate of 100hz.

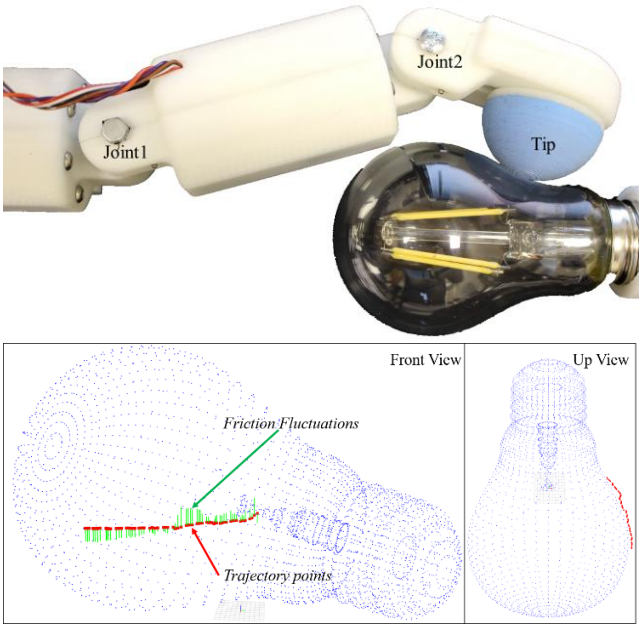

Fig. 1. Surface haptic exploration of an electric bulb (above) and geometry analysis (below). The blue point cloud denotes the object model, the dashed red lines denote the trajectory of contact points after the surface haptic exploration, and the green bars denote the variations of the friction coefficients. The height of the green bar is obtained by subtracting the mean of the friction coefficients $\bar{\mu}$ from that of the current contact location μ_c. Bars above the red lines mean larger than $\bar{\mu}$, and vice versa.

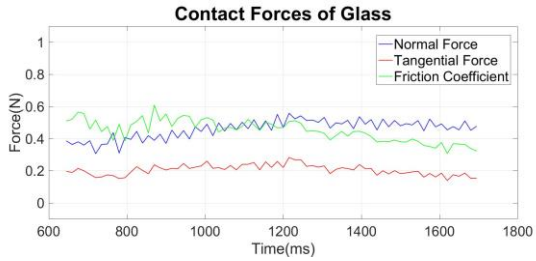

Fig. 2. Values of forces of one haptic exploration on the glass bulb, the mean and standard deviation of f_n is 0.45N and 0.06 respectively.

III. Object Recognition Algorithm

Using the aforementioned test platform, $\vec{\boldsymbol{F}}$ and T[$\overrightarrow{\boldsymbol{P_O}}$] will be obtained and stored after the surface haptic exploration. In order to combine this information, we developed an object recognition method using a multivariate Gaussian Bayesian classifier that recognizes the objects with the obtained data.

A. Features Calculation

To create the features for the classifier, $\vec{\boldsymbol{F}}$ and T[$\overrightarrow{\boldsymbol{P_O}}$] are interpolated into friction coefficients, surface roughness, and the geometry information. The friction coefficients are calculated using (1) for each data collected.

$$\mu = f_t / f_n \tag{1}$$

The mean $\bar{\mu}$ of all the friction coefficients (μ_1, μ_2, μ_3 ...) for one exploration is calculated as the friction feature. The variance σ^2 of the calculated friction coefficients is the feature indicating the surface roughness (due to the fact that the bigger the roughness is, the bigger the changes of the friction

This article has been accepted for publication in a future issue of this journal, but has not been fully edited. Content may change prior to final publication. Citation information: DOI 10.1109/LRA.2018.2814083, IEEE Robotics and Automation Letters

coefficients will be, we selected σ^2 as the roughness indicator). Green bars in Fig. 1 (below) denote the variations of the friction coefficients.

The geometry feature is computed by getting the fitting error of T[$\overrightarrow{\boldsymbol{P_O}}$] from the object's geometry file. Given the geometry data of an object O[$\overrightarrow{\boldsymbol{P}}$], the fitting error ε with T[$\overrightarrow{\boldsymbol{P_O}}$] can be calculated using ICP (Iterative Closest Point) [26] in PCL (Point Cloud Library). This method has limitations, since it requires the object's model to be provided beforehand, but this could be improved by using other features like mean curvature or scale of T[$\overrightarrow{\boldsymbol{P_O}}$] in the future. Moreover, in order to facilitate the ICP fitting, we rotate the robotic arm by a certain number of degrees after each exploration to get more geometric data of the object. Using the glass bulb as an example (see Fig. 1 below), the trajectory points obtained after surface haptic exploration match well with the surface of the bulb, and consequently the fitting error is low. If fitting the trajectory with the model of a different object, the fitting error will become larger, explaining that the fitting error can be used as a feature for recognizing the object.

B. *Features Calculation*

With the given three features, we observed that they all followed a Gaussian distribution, thus we decided to select the multivariate Gaussian function to combine all the three features. In detail, the distributions can be estimated using the parametric density function, which assumes that a continuous mathematical function can be fitted to a set of samples. Typically, the multivariate Gaussian function is used for such a purpose, giving rise to bell-like probability distributions. The mathematical expression for the multivariate Gaussian function is presented in (2). The equation describes the probability of a single variable and it shows that the mean of the studied variable and its standard deviation are needed [27]. In our case, the variable is a three-dimensional vector containing the three aforementioned features.

$$p(\vec{\boldsymbol{x}}|\omega_j) = \frac{1}{\sqrt{\det(\sum_c)\cdot(2\pi)^{d/2}}} exp(-0.5(\vec{\boldsymbol{x}} - \overrightarrow{\boldsymbol{m}})^T \sum_{\boldsymbol{c}}{}^{-1} (\vec{\boldsymbol{x}} - \overrightarrow{\boldsymbol{m}})) \quad (2)$$

, where $p(\vec{\boldsymbol{x}}|\omega_j)$ is the likelihood of measuring a feature vector $\vec{\boldsymbol{x}}$ given that the object has identity ω_j, d is the dimension of the column features vector, $\vec{\boldsymbol{x}} = [\bar{\mu}, \sigma^2, \varepsilon]^T$ is the measured features vector and $\overrightarrow{\boldsymbol{m}} = [m_1, m_2, m_3]^T$ is the corresponding mean features vector.

Moreover, the mean feature vectors for each object are computed as the average of the test samples gathered in the training stage using (3). In this paper, $n = 100$ samples were collected for each object, which will be shown later in the experiment section.

$$\overrightarrow{\boldsymbol{m}} = \left[\frac{1}{n}\sum_1^n \bar{\mu}_i, \frac{1}{n}\sum_1^n \sigma_i^2, \frac{1}{n}\sum_1^n \varepsilon_i\right] \quad (3)$$

Besides, the covariance matrix $\sum_c$ is in this case a 3x3 matrix defined as specified in (4), where $Var(\bar{\mu}) = \frac{1}{n}\sum_{i=1}^n (\bar{\mu}_i - m_1)^2$ represents the variance of $\bar{\mu}$ and $Covar(\bar{\mu}, \sigma^2) = \frac{1}{n}\sum_{i=1}^n (\bar{\mu}_i - m_1)(\sigma_i^2 - m_2)$ represents the covariance of $\bar{\mu}, \sigma^2$, the same for the others.

$$\sum_{\boldsymbol{c}} = \begin{bmatrix} Var(\bar{\mu}) & Covar(\bar{\mu}, \sigma^2) & Covar(\bar{\mu}, \varepsilon) \\ Covar(\sigma^2, \bar{\mu}) & Var(\sigma^2) & Covar(\sigma^2, \varepsilon) \\ Covar(\varepsilon, \bar{\mu}) & Covar(\varepsilon, \sigma^2) & Var(\varepsilon) \end{bmatrix} \quad (4)$$

To illustrate the concept, Fig. 3 shows an example of the 2D multivariate Gaussian distribution. We calculate the mean values and covariant matrix of the friction coefficient and surface roughness features with the real data of the sponge, and use MatLab to generate the distributions.

The method computes the likelihoods with the mean features vector $\overrightarrow{\boldsymbol{m}}$ of each object, and the elements of $\sum_{\boldsymbol{c}}{}^{-1}$ are parametrized by using $(a, b, c, d, e, f, g, h, i)$ which represent the 9 values of the inverse matrix. With the determinant $D = det(\sum_{\boldsymbol{c}})$being substituted in (2), the likelihood for all the learnt objects is found as a function of the measured features vector $\vec{\boldsymbol{x}}$. This means that after each training, the parameters for the classifier are updated once, and after they have been updated, they are used to recognize the objects. We think it could be better if we can continuously update the parameters even when we are doing the tests, which means the classifier can learn and evolve continuously. This will be discussed more in the future work section.

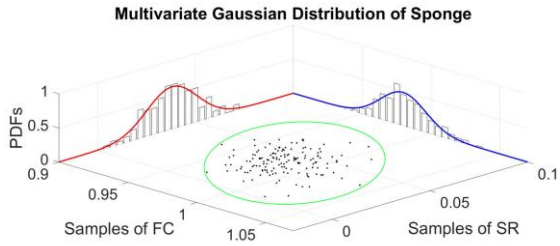

Fig. 3. Multivariate Gaussian distribution obtained with the data from the sponge. FC represents friction coefficients, SR represents surface roughness, PDF is the probability distribution function

C. *Recognize Objects through the Bayesian Decision Rule*

Once the system has computed the class-conditional probability distributions (likelihoods) for the objects, it will be used for object recognition with the input of the three features values in real time. The expression of the Bayesian decision rule is presented in (5). The object recognition is using an iterative way to compute the posterior probabilities for all the known objects after each surface haptic exploration. If none of the posterior probabilities exceeds a defined threshold ϑ, a new time's exploration will be carried out and use its previous posterior probabilities as new prior probabilities. The object recognition decides the object' identity when any of the posterior probabilities surpasses the threshold ϑ [22].

$$p(\omega_j|\overrightarrow{\boldsymbol{x_t}}) = \frac{p(\vec{\boldsymbol{x}}|\omega_j)\cdot p(\omega_j|\overrightarrow{\boldsymbol{x_{t-1}}})}{\sum_{j=1}^N [p(\vec{\boldsymbol{x}}|\omega_j)\cdot p(\omega_j|\overrightarrow{\boldsymbol{x_{t-1}}})]} \quad (5)$$

Where, $p(\omega_j|\overrightarrow{\boldsymbol{x_t}})$ is the probability that the object has identity ω_j given that it is measured to have features vector $\vec{\boldsymbol{x}}$ in time t ($Posterior_j$), $p(\vec{\boldsymbol{x}}|\omega_j)$ is the likelihood of measuring a features vector $\vec{\boldsymbol{x}}$ given that the object has identity ω_j, $p(\omega_j|\overrightarrow{\boldsymbol{x_{t-1}}})$ is the probability that the object has identity ω_j given that it is measured to have features vector $\vec{\boldsymbol{x}}$ in time $t-1$ ($Prior_j$).

This article has been accepted for publication in a future issue of this journal, but has not been fully edited. Content may change prior to final publication. Citation information: DOI 10.1109/LRA.2018.2814083, IEEE Robotics and Automation Letters

Algorithm 1 details the object recognition process.

Fig. 4 shows the classified result of three objects with different materials. Because it is difficult to show all three features in one figure, only the $\bar{\mu}, \sigma^2$ are shown, and for better expression, the values of the two features have been magnified respectively.

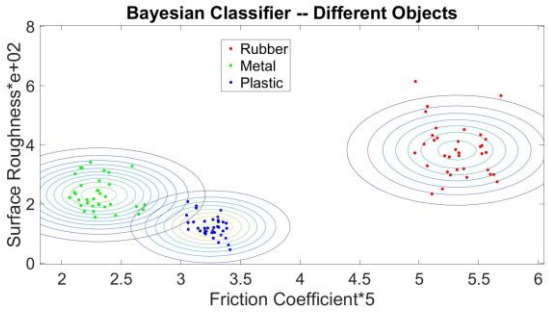

Fig. 4. The classification result with two features of rubber, metal and plastic. The points are constructed by from the values of the two features, and it can be seen that points of the rubber are distributed away from the other two while points of the metal and plastic are close to each other

Algorithm 1 Object recognition with proposed classifier

1: Initialise array of objects and load probability parameters, prior probabilities as 1/N, posterior probabilities as 0
2: **While** max $p(\omega_j|\overrightarrow{\boldsymbol{x_t}})< \vartheta$
3: **While** surface haptic exploration has not ended
4: **If** contact is occurring
5: Stack current $\vec{\boldsymbol{F}}$, $\overrightarrow{\boldsymbol{P_O}}$
6: **End if**
7: **End while**
8: Compute features vector $\vec{\boldsymbol{x}} = [\bar{\mu}, \sigma^2, \varepsilon]^T$
9: **For** each candidate object ω_j
10: Compute Likelihood value $p(\vec{\boldsymbol{x}}\,|\omega_j)$, Prior $p(\omega_j|\overrightarrow{\boldsymbol{x_{t-1}}})$
11: **End for**
12: Get Evidence $\sum_{j=1}^{N}[p(\vec{\boldsymbol{x}}|\omega_j)\cdot p(\omega_j|\overrightarrow{\boldsymbol{x_{t-1}}})]$
13: **For** each candidate object ω_j
14: Compute Posterior probability $p(\omega_j|\overrightarrow{\boldsymbol{x_t}})$
15: **End for**
16: Find maximum $p(\omega_j|\overrightarrow{\boldsymbol{x_t}})$
17: **End while**
18: Decide object's identity

IV. Experimental Evaluation

In order to verify the performance of the proposed object recognition method, experiments have been conducted. 18 daily-use objects shown in Fig. 5, have been tested. Since the object recognition algorithm relies on the surface friction coefficients, surface roughness and geometry property of the objects, the objects chosen for the experiments have various types of surface materials and geometries. We also selected a deformable object which has liquid inside (no.8), a soft object (no.12), objects with changing surface frictions (no.16, 17) and complex shaped objects (no.15, 18). For the geometry feature, we prepared all the 3D model files for the experimental objects. The 3D models of the objects can be obtained using 3D depth cameras (like Kinect camera) or from an existing database. Again, this has limitations and needs more research in the future. The algorithm calculates the ε of T$[\overrightarrow{\boldsymbol{P_O}}]$ with all the objects' 3D model data O$[\overrightarrow{\boldsymbol{P}}]$ after each exploration using PCL, and chooses ε as the geometry feature. Along with other features, the classifier was trained to recognize the objects. The procedure of the experiments is as follows:

- Decided the desired f_n and velocity v for the surface haptic exploration.
- Carried out 100 explorations for each object, and after each exploration, computed $\vec{\boldsymbol{x}} = [\bar{\mu}, \sigma^2, \varepsilon]^T$ and stored into the dataset. We did 20 times as a group with all objects and same desired f_n and v, different groups have different desired f_n or v.
- Constructed the multivariate Gaussian Bayesian classifier with the dataset.
- Repeated 50 object recognitions (10 times as a group for all objects) with changing desired f_n and v using the classifier for each object and recorded all the results.

The relative distance between the sensor and the object was not fixed. And we did the tests with all the objects in random orders after we trained the classifier. The recognition result was decided when the posterior probability is larger than the threshold ϑ set manually in the object recognition algorithm [22]. In our case, 0.9 was chosen as the threshold ϑ.

Fig. 5. The objects used for experiments, from no.1 to no.18 they are a metal plate, plastic lid, eraser, rubber, box, sponge, tape, grease, black ball, 3D printed ball, bulb, soft pad, glass bottle, coke can, 3D printed statue, spring, screw, computer mouse.

The $\bar{\mu}, \sigma^2$ of the sponge, eraser, black ball and tape are shown in Fig. 6 and it can be seen that the two features of the sponge and the tape are different in value; however, the eraser and the black ball have similar values making it difficult to classify them with only two features. Accordingly, we added the geometry feature. With all the three features, the recognition accuracies of the 18 objects are obtained and shown in Table I, and the overall average accuracy is 92.3%. During the test, we tried changing the desired f_n and v for each object, and noted that the overall accuracy was not affected by changing the configuration. These all present the high accuracy

This article has been accepted for publication in a future issue of this journal, but has not been fully edited. Content may change prior to final publication. Citation information: DOI 10.1109/LRA.2018.2814083, IEEE Robotics and Automation Letters

and robustness of the proposed method. However, it can be seen that the black rubber and sponge have relatively low recognition accuracy, which can be explained by them having similar friction coefficients, surface roughness and geometry. The values of the features of these two objects are shown in Table II, indicating the similarities. Also it will be difficult to distinguish object with small shape but different scale. This may be solvable by extending the exploration area, to calculate the scale of the object. These findings imply that the recognition accuracy could be improved by adding more dimensionality, like a stiffness feature, curvature feature or scale when the existing features are not enough for separating them. For different object, the key features that give us the most information for recognizing it are also different. This will be explored more in our future work.

TABLE. I

Name	Accuracy	Name	Accuracy
Metal plate	92%	White ball	92%
Plastic lid	92%	Bulb	94%
Eraser	92%	Soft pad	92%
Rubber	90%	Glass bottle	94%
Box	92%	Coke can	92%
Sponge	90%	Statue	94%
Tape	92%	Spring	92%
Grease	94%	Screw	92%
Black ball	92%	Mouse	94%
Average Accuracy: 92.3%			

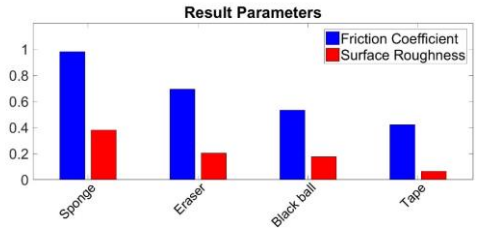

Fig. 6. Experiment results of two features for 4 different objects.

TABLE. II

Object	FC	SR	ICP
	1.041932	0.038321	0.465
	0.982132	0.037832	0.476

V. Discussion of the Proposed Classifier

Comparisons have been conducted with other classifiers, including RBF (Radial Basis Function) kernel SVM (Support Vector Machine), Gaussian Process, Random Forest, Multi-layer Perceptron classifier, AdaBoost, and the Quadratic Discriminant Analysis (QDA). We used the $\bar{\mu}$ *and* σ^2 data obtained from the experiments to do the comparisons. We separated them into 5 groups and each group has 3 objects. Fig. 7 shows the result of the classification comparison for one group including the metal plate, plastic box and the 3D printed plate, which have similar friction coefficients and surface roughness (refer to "Input data").

In our study, 120 data were used for training (40 for each object) and 60 data (20 for each) were used for testing the accuracy of each classifier. It can be seen from the figure of "Input data" that the data from the selected objects are located

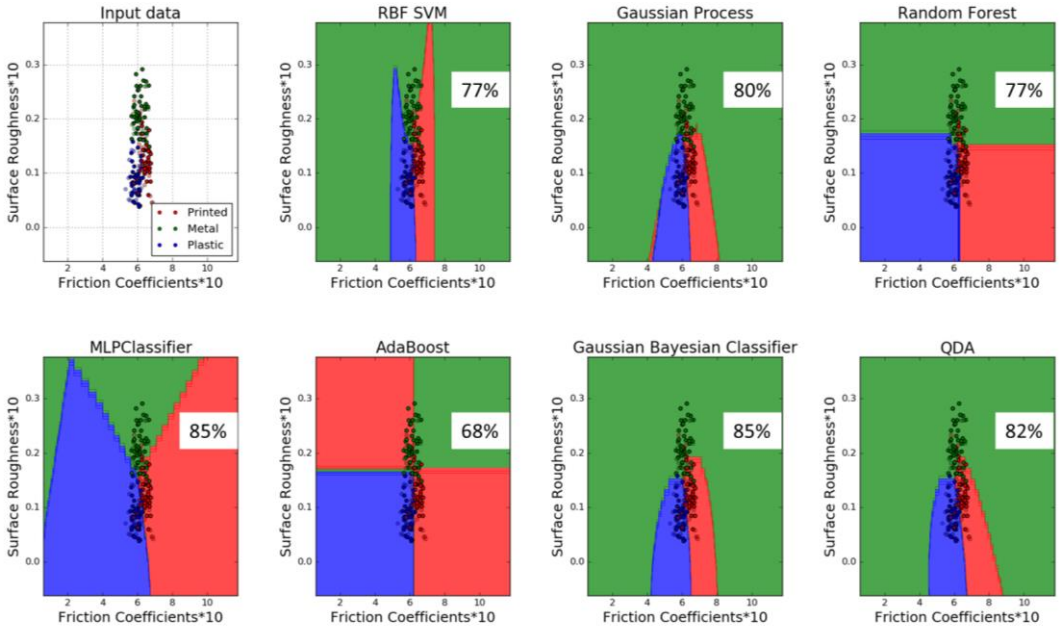

Figure. 7 The comparison of different classifiers using the data of friction coefficients and surface roughness from a 3D printed plate, and metal and plastic objects. The non-transparent points are the data for training and the translucent points are the test data; the numbers indicate the accuracy (percentage) of the classifiers; the colored areas in the figures denote the classification result, red for the printed plate, green for the metal plate, and blue for the plastic object.

close to each other due to their similar values. To make this comparison reasonable, all the other classifiers were using optimized parameters. The experimental results show that the Gaussian Bayesian classifier has high accuracy (refer to Fig. 7, which shows the result of one group) among other classifiers. This shows that the classifier is easier to implement having a high accuracy in classification with a limited amount of data.

The high accuracy is not the key reason of why we selected the classifier. Most importantly, Fig. 4 presents the distributions of the feature values of the three objects, which can be obtained continuously when new data are added and the classifier is able to show the process of classifying the objects. When the updated $p(\omega_j|\overrightarrow{x_t})$ is low, we can observe the similarities of the features with the multivariate Gaussian functions to find out if the features are adequate for recognition. With this platform, by re-planning the exploration accordingly to get necessary features data that provide the most information gain for recognition, the exploration can become more active and efficient for different unknown objects. For instance, the metal and plastic objects have similar friction coefficients and surface roughness, making it difficult to classify them; a new feature of geometry information was added accordingly.

VI. Conclusion and Future Work

There are some approaches that we can explore in the next steps. Firstly, the classifier can become more reliable if it can learn and evolve continuously, and this has not been actioned. This could be done if we can determine whether the data obtained are credible for training the classifier; then new data can be added continuously for training. Secondly, the proposed classifier can pave the way towards active exploration with some extensions: we used the ICP fitting error as one feature; however, because the object is not fixed, the trajectories of each exploration are not exactly the same, and each time only part of the geometry can be explored. Hence the fitting error is not precise enough for the classifier. It can be improved by exploring more paths on the object and selecting paths that can give us more information concerning the geometry of the object. Moreover, because the proposed classifier is traceable in recognizing the objects, we can add new dimensionality to the classifier and add decision rules to decide which features to use for specific objects for better recognition. For instance, we can change the exploration method to get stiffness data if other features are not enough for recognizing the object. All of these work together for active exploration, making the exploration and interaction more efficient, goal-oriented and adaptive.

References

[1] G. Robles-De-La-Torre, "The importance of the sense of touch in virtual and real environments," *IEEE Multimedia* vol.13, no. 3, pp. 24-30, Jul. 2006.

[2] T. J. Prescott, M. E. Diamond, and A. M. Wing. "Active touch sensing," *Phil. Trans. R. Soc. B* vol.366, no. 1581, pp. 2989-2995, Nov. 2011.

[3] A. D'Amore and M. Valle, *Robotic Tactile Sensing: Technologies and System*. New York, NY, USA: Springer, Jun. 2013.

[4] R.D.P. Wong, R.B. Hellman and V.J. Santos, "Haptic exploration of fingertip-sized geometric features using a multimodal tactile sensor," In *SPIE Sensing Technology+ Applications,* pp. 911605-911605, International Society for Optics and Photonics, June, 2014.

[5] R. Klatzky and C. L. Reed, "Haptic Exploration," In *Scholarpedia of Touch*, pp. 177-183, Atlantis Press, 2016.

[6] N. Wettels and G.E. Loeb, "Haptic feature extraction from a biomimetic tactile sensor: force, contact location and curvature," In *Robotics and Biomimetics (ROBIO), 2011 IEEE International Conference on* pp. 2471-2478, IEEE, December, 2011.

[7] A. M. Okamura, and M. R. Cutkosky, "Feature detection for haptic exploration with robotic fingers," *The International Journal of Robotics Research* vol. 20, no. 12, pp. 925-938, Dec. 2001.

[8] H. Liu, X. Song, J. Bimbo, L. Seneviratne, and K. Althoefer, "Surface material recognition through haptic exploration using an intelligent contact sensing finger," *2012 IEEE/RSJ International Conference on Intelligent Robots and Systems*, pp. 52-57, IEEE, Oct. 2012.

[9] Luo S, Mou W, Althoefer K, Liu H. Novel tactile-SIFT descriptor for object shape recognition. IEEE Sensors Journal. 2015 Sep;15(9):5001-9.

[10] Bimbo J, Luo S, Althoefer K, Liu H. In-hand object pose estimation using covariance-based tactile to geometry matching. IEEE Robotics and Automation Letters. 2016 Jan;1(1):570-7.

[11] D. S. Chathuranga, Z. Wang, Y. Noh, T. Nanayakkara, and S. Hirai, "Robust real time material classification algorithm using soft three axis tactile sensor: Evaluation of the algorithm," In *Intelligent Robots and Systems (IROS), 2015 IEEE/RSJ International Conference on*, pp. 2093-2098. IEEE, 2015.

[12] A. M. Okamura, M. L. Turner, and M. R. Cutkosky, "Haptic exploration of objects with rolling and sliding," In Robotics and Automation, 1997. Proceedings, 1997 IEEE International Conference on, vol. 3, pp. 2485-2490, IEEE, Apr. 1997.

[13] A. Spiers, M. Liarokapis, B. Calli, and A. Dollar, "Single-Grasp Object Classification and Feature Extraction with Simple Robot Hands and Tactile Sensors," *IEEE Transactions on Haptics,* vol. 9, no. 2, pp. 207-220, April-June 1, 2016.

[14] N. Jamali, and C. Sammut, "Majority voting: Material classification by tactile sensing using surface texture," IEEE Transactions on Robotics, vol. 27, no. 3, pp. 508-521, June. 2011.

[15] X. Song, H. Liu, K. Althoefer, T. Nanayakkara, and L. D. Seneviratne, "Efficient break-away friction ratio and slip prediction based on haptic surface exploration," IEEE Transactions on Robotics, vol. 30, no. 1, pp. 203-219, Feb. 2014.

[16] J. Martínez, A. García, M. Oliver, J. P. Molina, and P. González, "Identifying virtual 3D geometric shapes with a vibrotactile glove," IEEE computer graphics and applications, vol. 36, no. 1, pp. 42-51, 2016.

[17] P. K. Allen, and K. S. Roberts, "Haptic object recognition using a multi-fingered dextrous hand," Robotics and Automation, 1989. Proceedings, 1989 IEEE International Conference on, pp. 342-347, IEEE, May. 1989.

[18] J. Back, J. Bimbo, Y. Noh, L. Seneviratne, K. Althoefer, and H. Liu, "Control a contact sensing finger for surface haptic exploration," 2014 IEEE International Conference on Robotics and Automation (ICRA), pp. 2736-2741, IEEE, May. 2014.

[19] M. Gabardi, M. Solazzi, D. Leonardis, and A. Frisoli, "A new wearable fingertip haptic interface for the rendering of virtual shapes and surface features," 2016 IEEE Haptics Symposium (HAPTICS), pp. 140-146, IEEE, Apr. 2016.

[20] H. Gu, S. Fan, H. Zong, M. Jin and H. Liu, "Haptic Perception of Unknown Object by Robot Hand: Exploration Strategy and Recognition Approach," *International Journal of Humanoid Robotics*, vol.13(03), p.1650008, 2016.

[21] U. Martinez-Hernandez, T.J. Dodd, M.H. Evans, T.J. Prescott and N.F. Lepora, "Active sensorimotor control for tactile exploration," *Robotics and Autonomous Systems*, vol. *87*, pp.15-27, 2017.

[22] N. F. Lepora, U. Martinez-Hernandez, & T. J. Prescott, "Active Bayesian Perception for Simultaneous Object Localization and Identification," In Robotics: Science and Systems, 2013.

[23] R. S. Jamisola, P. Kormushev, A. Bicchi, and D. G. Caldwell, "Haptic exploration of unknown surfaces with discontinuities," In 2014 IEEE/RSJ International Conference on Intelligent Robots and Systems, pp. 1255-1260, IEEE, Sep. 2014.

[24] R. Martins, J. F. Ferreira, and J. Dias, "Touch attention Bayesian models for robotic active haptic exploration of heterogeneous surfaces," In 2014 IEEE/RSJ International Conference on Intelligent Robots and Systems, pp. 1208-1215, IEEE, Sep. 2014.

[25] H. Liu, K.C. Nguyen, V. Perdereau, J. Bimbo, J. Back, M. Godden, L.D. Seneviratne and K. Althoefer, "Finger contact sensing and the application in dexterous hand manipulation," Autonomous Robots, vol. 39, no. 1, pp.25-41, 2015.

[26] P. J. Besl and N. D. McKay, "A method for registration of 3-D shapes," *IEEE Trans. Pattern Anal. Mach. Intell.*, vol. 14, no. 2, pp. 239–256, Feb. 1992.

[27] C. M. Bishop, "Pattern recognition," *Machine Learning* 128, 2006.